

## Supplementary Methods

### Identifying somatic mutations in primary tumor tissue

Sequencing analysis of the primary tumor was performed using three different platforms for each set of patients with colorectal cancer (CRC). Tumor samples from 11, 27, and 14 patients were analyzed for Sets 1, 2, and 3, respectively. In Set 1, three regions of the primary tumor and corresponding DNA from peripheral blood mononuclear cells (PBMCs) (four samples) were analyzed to assess the effect of intra-tumor genetic heterogeneity on circulating tumor DNA (ctDNA) in our previous study (Ref. 33 of the main text). That study revealed that tumor genetic heterogeneity did not appear to represent a major obstacle for ctDNA analysis provided that a somatic mutation having a sufficient variant allele frequency (VAF) was selected from a single region of the tumor. Furthermore, commonly detected mutations among the three tumor regions were limited to several genes, such as *TP53*, *APC*, *KRAS*, *PIK3CA*, *FBXW7*, and *BRAF*.

To reduce costs and improve mutation detection efficiency of tumor sequencing, the pairing between tumor and PBMC-DNA (two DNA samples) was analyzed for Set 2 samples using a customized panel targeting 39 genes specific for CRC using an Ion Proton™ system (Thermo Fisher Scientific, Waltham, MA). Amplicon sequencing followed by identification of somatic mutations using the Ion Reporter software 5.0 tumor-normal workflow (Thermo Fisher Scientific) was performed as previously described (Refs. 32 and 34 of the main text). The following criteria were used as cutoffs: (1) total coverage >200, (2) variant coverage >10, and (3) variant frequency >10%. Mutations were subsequently called if they occurred in <0.1% of the reads in the normal control (minor allele frequency) and were absent from the dbSNP and 1000 Genomes Project database.

Considering the high mutation detection efficiency of tumor sequencing using the customized panel for Set 2, we analyzed only tumor DNA samples from a single region for Set 3 using an Ion S5™ system (Thermo Fisher Scientific). In Set 3, alignment to reference genomes and sequencing read counting were performed with Torrent Suite version 5.0 (Thermo Fisher Scientific), Hisat2 (<https://ccb.jhu.edu/software/hisat2/index.shtml>), and BWA (Burrows–Wheeler Alignment tool). In such cases, commonly-detected mutations among the three algorithms were prioritized in the subsequent mutation selection. The following criteria were used as cutoffs: (1) total coverage >200, (2) variant coverage >10, and (3) variant frequency >10%. Mutations were selected as with Set 2. Furthermore, mutations were called if they also occurred with minor allele frequencies (MAF < 0.01) in the Japanese SNP database

of the Tohoku Medical Megabank Organization (ToMMo).<sup>1</sup> Moreover, the same mutations shared among more than 3 of 14 patients in Set 3 were excluded from mutation selection when they did not frequently occur in CRC given the high likelihood that they resulted from sequence errors. For insertion and deletion mutations, the following criteria were used as cutoffs: (1) total coverage > 200; (2) variant coverage > 10; and (3) variant frequency > 20%. For Set 3, the dPCR probe/premier set for each specific mutation was designed after confirming that Sanger sequencing detected the mutation in tumor DNA and but not PBMC DNA.

### **Criteria for mutation selection in ctDNA assay using digital PCR**

According to our previous studies, between 1 and 5 mutations having VAFs >10% that were found in primary tumors were prioritized for digital PCR (dPCR) analysis (References 32-35 of the main text). The criteria used to select mutations for ctDNA assay were: (1) the mutation having the highest VAF in the primary tumor; (2) up to four additional mutations having a VAF >10% in the primary tumors; (3) recurrent mutations observed among patients; (4) mutated genes having a high success rate for primer/probe validation; and (5) exclusion of mutations with a surrounding sequence suspected of having low PCR efficiency and low specificity of hybridized probes (e.g., self-complementarity and/or secondary structure of the primer/probe). Furthermore, those mutations that were already validated in the tumor DNA from CRC or other types of malignancies could reduce the temporary cost and time needed for syntheses of specifically-designed probes for each tumor-specific mutation. Therefore, mutations listed in our dPCR primer/probe library and commercially available primer/probe sets (Quantdetect, Inc, Tokyo, Japan) were analyzed, even if the mutations detected in the primary tumors did not satisfy the criteria for mutation selection.

### **Definitions of ctDNA positivity and negativity in dPCR assays**

As previously described (References 32-35 of the main text), dPCR was performed using the QuantStudio3D Digital PCR system (Thermo Fisher Scientific). After PCR amplification, chips were read on a QuantStudio 3D Digital PCR Instrument (Thermo Fisher Scientific), and a secondary analysis was performed using QuantStudio 3D Analysis Suit Cloud software (Thermo Fisher Scientific). For further quality control, the boundaries of FAM, VIC, and undetermined events were manually defined. After confirmation of sufficiently separate reactions of both wild-type and mutant alleles in tumor DNA, plasma DNA was evaluated by dPCR. Plasma samples having more than two positive reactions (i.e., dots) for mutant DNA were defined as ctDNA-positive. If

only one positive reaction for mutant DNA was detected, samples were considered to be ctDNA-positive when more than one positive reaction for mutant DNA could be repeatedly detected upon retesting of the same sample. The VAF values were calculated as the fraction of mutant/(mutant + wild) divided by the number of partitions in which either the mutant or wild-type sequence was detected.<sup>2</sup> If no mutant partitions were detected, the case DNA was regarded as “negative”.

## References

1. Okuda H, Okamoto K, Abe M, et al. Correction to: Genome-wide association study identifies new loci for albuminuria in the Japanese population. *Clin Exp Nephrol* 2021;25:565.
2. Huggett JF, Foy CA, Benes V, et al. The digital MIQE guidelines: Minimum Information for publication of Quantitative digital PCR Experiments. *Clin Chem* 2013;59:892-902.

**Supplementary Table 1. Clinicopathological characteristics of patients in the study cohort.**

Patient No.	Age range	Sex	Primary tumor location	Size (mm <sup>2</sup> )	UICC stage <sup>a</sup>					Preoperative metastatic organ
					T	depth	N	M	pStage <sup>b</sup>	
CC16001	71-75	Female	Cecum	47×60	4a	SE	1a	0	IIIB	-
CC16002	81-85	Female	Cecum	57×35	3	SS	0	0	II	-
CC16003	51-55	Female	Rectum	23×22	3	SS	2	0	IIIB	-
CC16005	71-75	Female	Rectosigmoid	22×20	2	MP	1b	0	IIIA	-
CC16006	51-55	Male	Sigmoid	9×11	1b	SM	0	0	I	-
CC16008	71-75	Female	Cecum	26×20	2	MP	1b	0	IIIA	-
CC16009	86-90	Female	Rectum	60×75	4a	SE	0	0	II	-
CC16010	56-60	Female	Rectum	35×70	4a	AI	2b	1a	IVB	Liver
CC16011	51-55	Female	Sigmoid	37×48	4a	SE	1a	1a	IVA	LN <sup>c</sup>
CC16012	56-60	Female	Sigmoid	53×49	3	SS	0	0	II	-
CC16013	76-80	Female	Rectum	65×50	3	SS	0	0	II	-
CC16014	51-55	Female	Rectum	85×57	3	SS	0	0	II	-
CC16015	71-75	Male	Sigmoid	9×11	4b	SM	0	0	IIC	-
CC16016	51-55	Male	Sigmoid	28×28	3	SS	1a	0	IIIB	-
CC16017	76-80	Female	Ascending	103×72	3	SS	1b	0	IIIA	-
CC16018	81-85	Male	Ascending	42×30	3	SS	X	0	IIA	-
CC16019	71-75	Male	Transverse	110×103	4a	SE	0	0	IIB	-
CC16020	71-75	Female	Sigmoid	35×70	3	SS	1a	0	IIIB	-
CC16021	71-75	Male	Ascending	39×42	3	SS	0	0	IIA	-
CC16022	56-60	Male	Rectum	50×42	2	MP	0	0	I	-
CC16023	81-85	Female	Cecum	55×82	3	SS	2b	0	IIC	-
CC16024	36-40	Female	Rectum	61×45	3	SS	0	0	IIA	-
CC16025	71-75	Male	Ascending	37×26	3	SS	0	0	IIA	-
CC16026	76-80	Female	Ascending	58×49	3	SS	0	0	IIA	-
CC16027	76-80	Female	Ascending	34×29	3	SS	1	0	IIIA	-
CC16028	51-55	Female	Sigmoid	20×17	2	MP	0	0	I	-
CC16029	56-60	Female	Sigmoid	46×42	3	SS	1a	0	IIIB	-
CC16030	66-70	Male	Ascending	17×20	3	SS	1b	0	IIIB	-
CC16031	76-80	Male	Sigmoid	33×30	1	CIS	0	0	I	-

CC16032	71-75	Female	Ascending	73×63	4a	SE	1b	0	IIIB	-
CC16034	76-80	Female	Sigmoid	43×60	3	SS	1a	0	IIIB	-
CC16035	61-65	Male	Rectum	21×17	3	SS	2a	0	IIIB	-
CC16036	81-85	Female	Cecum	27×26	2	1b	0	0	IIIA	-
CC16037	51-55	Female	Sigmoid	58×32	3	SS	0	0	IIA	-
CC16038	61-65	Male	Ascending	32×26	3	SS	0	0	IIA	-
CC16039	81-85	Male	Transverse	27×26	3	SS	0	0	IIA	-
CC16040	71-75	Female	Sigmoid	25×22	3	SS	0	0	IIA	-
CC16041	66-70	Male	Rectum	35×42	3	SS	2a	0	IIIB	-
CC16042	66-70	Female	Sigmoid	54×33	3	SS	2a	0	IIIB	-
CC16043	56-60	Female	Transverse	47×28	3	SS	2a	0	IIIB	-
CC16044	71-75	Male	Rectum	52×35	3	SS	0	0	IIA	-
CC16046	75-80	Male	Sigmoid	40×37	3	SS	0	0	IIA	-
CC16047	66-70	Female	Rectum	57×32	3	SS	0	0	IIA	-
CC16048	66-70	Female	Sigmoid	58×32	3	SS	0	0	IIA	-
CC16049	81-85	Female	Sigmoid	53×52	3	SS	0	0	IIA	-
CC16050	66-70	Female	Transverse	47×30	3	SS	0	0	IIA	-
CC16051	66-70	Female	Rectum	88×62	3	SS	0	0	IIA	-
CC16054	66-70	Male	Ascending	35×55	3	SS	1a	0	IIIB	-
CC16056	56-60	Male	Rectum	43×60	4b	SE	2b	0	IIIC	-
CC16057	61-65	Male	Transverse	35×52	4b	SE	2a	0	IIIC	-
CC16058	66-70	Male	Rectum	63×48	3	SS	0	0	IIA	-
CC16060	61-65	Male	Rectum	80×100	3	SS	0	0	IIA	-

<sup>a</sup> TNM classification, 8th edition<sup>b</sup> Pathological stage<sup>c</sup> Nonregional abdominal para-aortic lymph nodes

**Supplementary Table 2. List of genes in the customized panel for CRC.**

<i>ACVR2A</i>	<i>DKK2</i>	<i>NRAS</i>
<i>AMER1</i>	<i>DKK3</i>	<i>PIF1</i>
<i>APC</i>	<i>DKK4</i>	<i>PIK3CA</i>
<i>ARID1A</i>	<i>FBXW7</i>	<i>PTEN</i>
<i>ATM</i>	<i>FZD3</i>	<i>RBL1</i>
<i>AXIN2</i>	<i>FZD10</i>	<i>RNF43</i>
<i>BMP4</i>	<i>GNAS</i>	<i>SMAD4</i>
<i>BRAF</i>	<i>GSK3B</i>	<i>SOX9</i>
<i>CDKN2A</i>	<i>HRAS</i>	<i>TCF7L2</i>
<i>CHD7</i>	<i>KRAS</i>	<i>TELO2</i>
<i>CHD8</i>	<i>LRP5</i>	<i>TGFBR2</i>
<i>CTNNB1</i>	<i>MLH1</i>	<i>TP53</i>
<i>DKK1</i>	<i>MSH6</i>	<i>XAF1</i>

**Supplementary Table 3. Primary tumor mutations detected through sequence analysis of Set 2 samples using Ion Proton™ and circulating tumor DNA levels (ctDNA) measured by digital PCR.**

Case ID	Chromosomal location	Gene	Variant type	Base change	Amino acid change	Total allele	Wild type	Mutant allele	Primary VAF <sup>a</sup> (%)	dPCR <sup>b</sup>	pre ctDNA <sup>c</sup> (%)
CC16002	chr12:25398280	KRAS	missense	c.37G>T	p.G13C	1995	1790	205	10.3	yes	0
	chrX:63411678	AMER1	nonsense	c.1489C>T	p.R497*	1997	1385	612	30.6		
CC16003	chr5:112175639	APC	nonsense	c.4348C>T	p.R1450*	1999	1021	978	48.9		
	chr17:7578256	TP53	nonsense	c.586C>T	p.R196*	1948	1025	923	47.4	yes	0.43
CC16006	chr14:21868397	CHD8	missense	c.4640A>G	p.H1547R	1998	1586	412	20.62		
	chr12:25398283	KRAS	missense	c.34G>T	p.G12C	1998	1779	218	10.91	yes	0
	chr17:7578368	TP53	splicesite_3	c.559+3G>C		1920	1543	376	19.6		
CC16009	chr17:63554007	AXIN2	frameshift deletion	c.731delC	p.S244fs	1991	1228	763	38.3		
	chr12:25398283	KRAS	missense	c.35G>A	p.G12D	1997	1459	538	26.9	yes	0.25
	chr2:48027519	MSH6	missense	c.2397G>A	p.M799I	2000	1677	323	16.2		
	chr17:7578368	TP53	splicesite_3	c.559+3G>C		1910	1274	635	33.2		
CC16017	chr5:112175639	APC	nonsense	c.4348C>T	p.R1450*	1996	1081	915	45.8		
	chr5:112173914	APC	nonsense	c.2623A>T	p.K875*	1999	1167	832	41.6		
	chr3:41278106	CTNNB1	missense	c.1982G>T	p.R661L	1998	1101	897	44.9		
	chr12:25378561	KRAS	missense	c.437C>T	p.A146V	1550	869	681	43.9		

	chr1:115258745	NRAS	missense	c.37G>C	p.G13R	2000	1492	506	25.3		
	chr3:178936082	PIK3CA	missense	c.1624G>A	p.E542K	1318	1017	301	22.8	yes	0
CC16018	chr5:112175672	APC	frameshift deletion	c.4391_4394delAGAG	p.E1464fs	1949	1525	423	21.70		
	chr5:112174631	APC	nonsense	c.3340C>T	p.R1114*	1999	1589	410	20.51		
CC16019	chr17:7577546	TP53	missense	c.733G>A	p.G245S	1993	1421	570	28.60	yes	0.18
	chr7:140453133	BRAF	missense	c.1799T>A	p.V600E	1980	1632	347	17.53	yes	11.9
CC16020	chr17:7577120	TP53	missense	c.818G>A	p.R273H	1966	1165	801	40.74	yes	4.57
	chr5:112151261	APC	missense	c.904C>T	p.R302*	1998	1107	891	44.59	yes	0.17
CC16021	chr17:7578474	TP53	missense	c.451C>G	p.P151A	1616	809	803	49.69	yes	0.75
	chr7:140453155	BRAF	missense	c.1780G>C	p.D594H	1991	1507	484	24.31	yes	0
CC16022	chr20:57485014	GNAS	missense	c.848G>A	p.R283H	1998	1556	442	22.12		
	chr12:25378562	KRAS	missense	c.436G>A	p.A146T	1999	1762	237	11.86		
CC16024	chr5:112128203	APC	nonsense	c.706C>T	p.Q236*	1999	1612	387	19.36		
	chr4:153247376	FBXW7	nonframeshift deletion	c.1423_1425delGTT	p.V475del	1984	1114	870	43.85		
	chr4:153332760	FBXW7	frameshift insertion	c.195_196insGA	p.P66fs	1997	1522	475	23.79		
	chr12:25398280	KRAS	missense	c.38G>A	p.G13D	1997	1050	944	47.27	yes	0.55
	chr17:7578474	TP53	missense	c.451C>A	p.P151T	1978	782	1194	60.36		
CC16024	chr2:148683611	ACVR2A	nonsense	c.1228G>T	p.E410*	1893	1278	615	32.49		

chr5:112175046	APC	missense	c.3755C>A	p.S1252Y	1914	862	653	34.12		
chr1:27106178	ARID1A	nonsense	c.5789C>A	p.S1930*	1092	807	285	26.10		
chr11:108202715	ATM	missense	c.7739G>T	p.R2580I	1997	1418	579	28.99		
chr11:108196939	ATM	missense	c.6962C>T	p.A2321V	1998	1471	527	26.38		
chr14:21871721	CHD8	missense	c.3409C>A	p.L1137I	1999	1461	538	26.91		
chr14:21860965	CHD8	missense	c.6472C>T	p.R2158C	1993	1491	502	25.19		
chr3:41277291	CTNNB1	missense	c.1760G>A	p.R587Q	1998	1352	646	32.33		
chr3:41266232	CTNNB1	nonsense	c.229G>T	p.E77*	1994	1441	553	27.73		
chr8:42231798	DKK4	missense	c.495T>G	p.I165M	1431	1172	259	18.10		
chr4:153244184	FBXW7	missense	c.1973G>A	p.R658Q	1977	1405	572	28.93		
chr4:153332915	FBXW7	missense	c.41G>A	p.R14Q	1979	1463	516	26.07		
chr12:130648241	FZD10	missense	c.754G>A	p.D252N	1991	1407	584	29.33		
chr12:130648713	FZD10	missense	c.1226G>A	p.G409D	1999	1457	542	27.11		
chr12:130647576	FZD10	missense	c.89G>A	p.G30D	1844	1509	335	18.17		
chr3:119624687	GSK3B	missense	c.728C>T	p.A243V	694	507	187	26.95		
chr2:48027661	MSH6	nonsense	c.2539G>T	p.E847*	203	129	74	36.45	yes	0
chr3:178916716	PIK3CA	nonsense	c.103G>T	p.E35*	1391	972	419	30.12		
chr3:178922301	PIK3CA	missense	c.1070G>A	p.R357Q	2000	1446	554	27.70		
chr3:178916642	PIK3CA	missense	c.29T>G	p.L10R	2000	1593	407	20.35		

	chr10:89692895	PTEN	missense	c.389G>A	p.R130Q	1972	1462	510	25.86		
	chr17:56435626	RNF43	missense	c.1511A>G	p.D504G	1999	1729	270	13.51		
	chr18:48603033	SMAD4	missense	c.1334G>A	p.R445Q	1402	1023	379	27.03		
	chr17:6676434	XAF1	missense	c.852G>T	p.E284D	365	304	61	16.71		
CC16025	chrX:63410048	AMER1	missense	c.3119C>A	p.A1040D	2000	1773	227	11.35	yes	0
	chr20:57484420	GNAS	missense	c.601C>T	p.R201C	1999	1441	558	27.91		
	chr12:25378562	KRAS	missense	c.436G>A	p.A146T	1999	590	1409	70.49		
CC16028	chr3:178936091	PIK3CA	missense	c.1633G>A	p.E545K	1999	1161	838	41.92	yes	0
	chr10:114912175	TCF7L2	frameshift deletion	c.1247delG	p.G416fs	1991	946	1045	52.49		
	chr17:7578443	TP53	missense	c.476C>T	p.A159V	1932	596	1336	69.15		
	chr5:112173917	APC	nonsense	c.2626C>T	p.R876*	2000	1535	465	23.25	yes	0
CC16029	chr5:112175628	APC	frameshift deletion	c.4338delT	p.Q1447fs	1987	1533	454	22.85		
	chr4:153258983	FBXW7	nonsense	c.832C>T	p.R278*	1653	1285	368	22.26		
	chr17:7578490	TP53	nonsense	c.438G>A	p.W146*	1824	1203	621	34.05		
	chrX:63411969	AMER1	nonsense	c.1198G>T	p.E400*	1568	484	1084	69.13		
	chr5:112176020	APC	nonsense	c.4729G>T	p.E1577*	959	633	326	33.99		
CC16030	chr5:112173736	APC	frameshift Insertion	c.2454_2455insTGGCAAC	p.M819fs	1996	1641	355	17.79		
	chr12:25378561	KRAS	missense	c.437C>T	p.A146V	1993	728	1265	63.47	yes	0.51
	chr10:89720665	PTEN	nonsense	c.821G>A	p.W274*	212	122	90	42.45		

	chr17:7577021	<i>TP53</i>	nonsense	c.916C>T	p.R306*	2000	1100	900	45.00	yes	0
CC16031	chr17:70117936	<i>SOX9</i>	missense	c.404T>A	p.L135H	1997	1762	235	11.77	yes	0.06
CC16036	chrX:63412020	<i>AMER1</i>	nonsense	c.1147G>T	p.E383*	1999	1385	614	30.72		
	chr5:112174682	<i>APC</i>	nonsense	c.3391C>T	p.Q1131*	1998	1629	369	18.47		
	chr12:25398280	<i>KRAS</i>	missense	c.38G>A	p.G13D	1996	1534	462	23.15	yes	0.22
	chr11:68179025	<i>LRP5</i>	missense	c.2440G>A	p.A814T	1994	1754	240	12.04		
	chr3:178936094	<i>PIK3CA</i>	missense	c.1636C>A	p.Q546K	545	408	137	25.14		
	chr17:7577156	<i>TP53</i>	splicesite_5	c.783-1G>A		1972	1348	624	31.64		
	chr5:112170648	<i>APC</i>	nonsense	c.1744G>T	p.E582*	2000	1680	320	16.00		
CC16037	chr17:7577556	<i>TP53</i>	missense	c.722C>G	p.S241C	1978	1187	788	39.84	yes	0.27
CC16038	chr12:25398280	<i>KRAS</i>	missense	c.38G>A	p.G13D	1998	1822	176	8.81	yes	0
CC16039	chr15:65116026	<i>PIF1</i>	missense	c.509C>T	p.T170M	813	656	157	19.31		
	chr17:7577553	<i>TP53</i>	frameshift Insertion	c.714_715insGT	p.N239fs	1492	666	825	55.29	yes	0
	chr5:112173917	<i>APC</i>	nonsense	c.2626C>T	p.R876*	1997	857	1140	57.09	yes	0
	chr1:27107138	<i>ARID1A</i>	frameshift deletion	c.6750delG	p.E2250fs	1998	1231	767	38.39		
CC16040	chr12:25398283	<i>KRAS</i>	missense	c.35G>A	p.G12D	1999	1255	744	37.22	yes	13.2
	chr3:178936095	<i>PIK3CA</i>	missense	c.1637A>G	p.Q546R	697	273	424	60.83		
	chr17:7578256	<i>TP53</i>	missense	c.584T>C	p.I195T	1949	797	1152	59.11		

CC16044	chr5:112116592	<i>APC</i>	nonsense	c.637C>T	p.R213*	1687	727	960	56.91	yes	1.73
	chr4:153249511	<i>FBXW7</i>	missense	c.1267G>A	p.G423R	1998	1280	718	35.94		
CC16046	chr5:112173718	<i>APC</i>	frameshift deletion	c.2428delA	p.R810fs	1995	1195	800	40.10		
	chr5:112128141	<i>APC</i>	splicesite_5	c.646-2A>G		1065	668	397	37.28		
	chr12:25398283	<i>KRAS</i>	missense	c.35G>A	p.G12D	1997	1209	784	39.26	yes	0
	chr3:178952085	<i>PIK3CA</i>	missense	c.3140A>G	p.H1047R	1999	1210	788	39.42	yes	0.84
CC16047	chr5:112128143	<i>APC</i>	nonsense	c.646C>T	p.R216*	1083	393	690	63.71		
	chr15:65112165	<i>PIF1</i>	missense	c.1214G>A	p.R405H	1905	1357	548	28.77		
	chr3:178936091	<i>PIK3CA</i>	missense	c.1633G>A	p.E545K	671	452	219	32.64	yes	0
CC16048	chr7:140453133	<i>BRAF</i>	missense	c.1799T>A	p.V600E	1979	881	1096	55.38	yes	0
	chr4:153258983	<i>FBXW7</i>	nonsense	c.832C>T	p.R278*	1999	1243	756	37.82		
	chr12:130648458	<i>FZD10</i>	missense	c.971C>T	p.S324L	2000	1229	771	38.55		
	chr17:7579348	<i>TP53</i>	frameshift deletion	c.338delT	p.F113fs	1992	1266	724	36.35		
CC16049	chr12:25398283	<i>KRAS</i>	missense	c.35G>T	p.G12V	2000	1250	747	37.35	yes	0
	chr17:7577528	<i>TP53</i>	missense	c.742C>T	p.R248W	1963	576	1386	70.61		
CC16050	chr5:112174580	<i>APC</i>	nonsense	c.3289G>T	p.E1097*	1997	1214	783	39.21		
	chr14:21876575	<i>CHD8</i>	nonsense	c.2626C>T	p.R876*	1997	882	1115	55.83		
	chr4:153247367	<i>FBXW7</i>	nonsense	c.1435C>T	p.R479*	1765	1210	555	31.44		

chr17:70117938	SOX9	missense	c.406A>G	p.S136G	2000	738	1262	63.10		
chr17:7577580	TP53	missense	c.701A>G	p.Y234C	1980	534	1446	73.03	yes	0

<sup>a</sup> Variant allele frequency

<sup>b</sup> Plasma DNA was evaluated by dPCR

<sup>c</sup> Pretreatment circulating tumor DNA

**Supplementary Table 4. Primary tumor mutations detected through sequence analysis of Set 3 using Ion 5S™ and circulating tumor DNA (ctDNA) levels measured by digital PCR.**

Case ID	Chromosomal location	Gene	Variant type	Base change	Amino acid change	Total allele	Wild type	Mutant allele	Primary VAF <sup>a</sup> (%)	dPCR <sup>b</sup>	pre ctDNA <sup>c</sup> (%)
CC16010	chr17:7675108	<i>TP53</i>	frameshift insertion	c.107_108insAGCA	p.H36Qfs*14	4610	2983	981	21.11	yes	8.54
	chr5:112839729	<i>APC</i>	stopgain	c.G4135T	p.E1379*	3959	2075	1880	47.49		
	chr12:25245350	<i>KRAS</i>	nonsynonymous	c.G35T	p.G12V	7680	3872	3802	49.51	yes	0.51
	chr20:37035354	<i>RBL1</i>	frameshift insertion	c.776dupC	p.S260Ffs*6	4520	3858	1198	23.58		
	chr17:7675232	<i>TP53</i>	nonsynonymous	c.C380A	p.S127Y	3021	605	2384	78.91	yes	0.19
CC16012	chr11:108335029	<i>ATM</i>	nonsynonymous	c.C8071T	p.R2691C	3427	2342	983	29.53		
	chr7:140753336	<i>BRAF</i>	nonsynonymous	c.T1799A	p.V600E	5149	3438	1697	32.95	yes	0
	chr20:58855061	<i>GNAS</i>	nonsynonymous	c.G1796A	p.R599H	4196	2611	1576	37.55		
	chr3:179234297	<i>PIK3CA</i>	nonsynonymous	c.A3140G	p.H1047R	5276	3295	1969	37.26	yes	0
	chr17:58362564	<i>RNF43</i>	nonsynonymous	c.C667T	p.R223C	2587	1341	1245	48.13		
	chr10:113165642	<i>TCF7L2</i>	frameshift deletion	c.1411delC	p.S473Pfs*5	2148	1442	671	30.74		
	chr5:112839693	<i>APC</i>	frameshift insertion	c.4046dupA	p.T1350Dfs*7	2540	1707	837	32.66	yes	8.3
CC16014	chr14:21393628	<i>CHD8</i>	nonsynonymous	c.G6167A	p.R2056Q	2700	1565	1112	41.12		
	chr17:7675131	<i>TP53</i>	nonsynonymous	c.G481A	p.A161T	2370	1545	814	34.39	yes	8.68
CC16015	chr11:108229288	<i>ATM</i>	nonsynonymous	c.G296A	p.S99N	2630	2047	558	21.17		

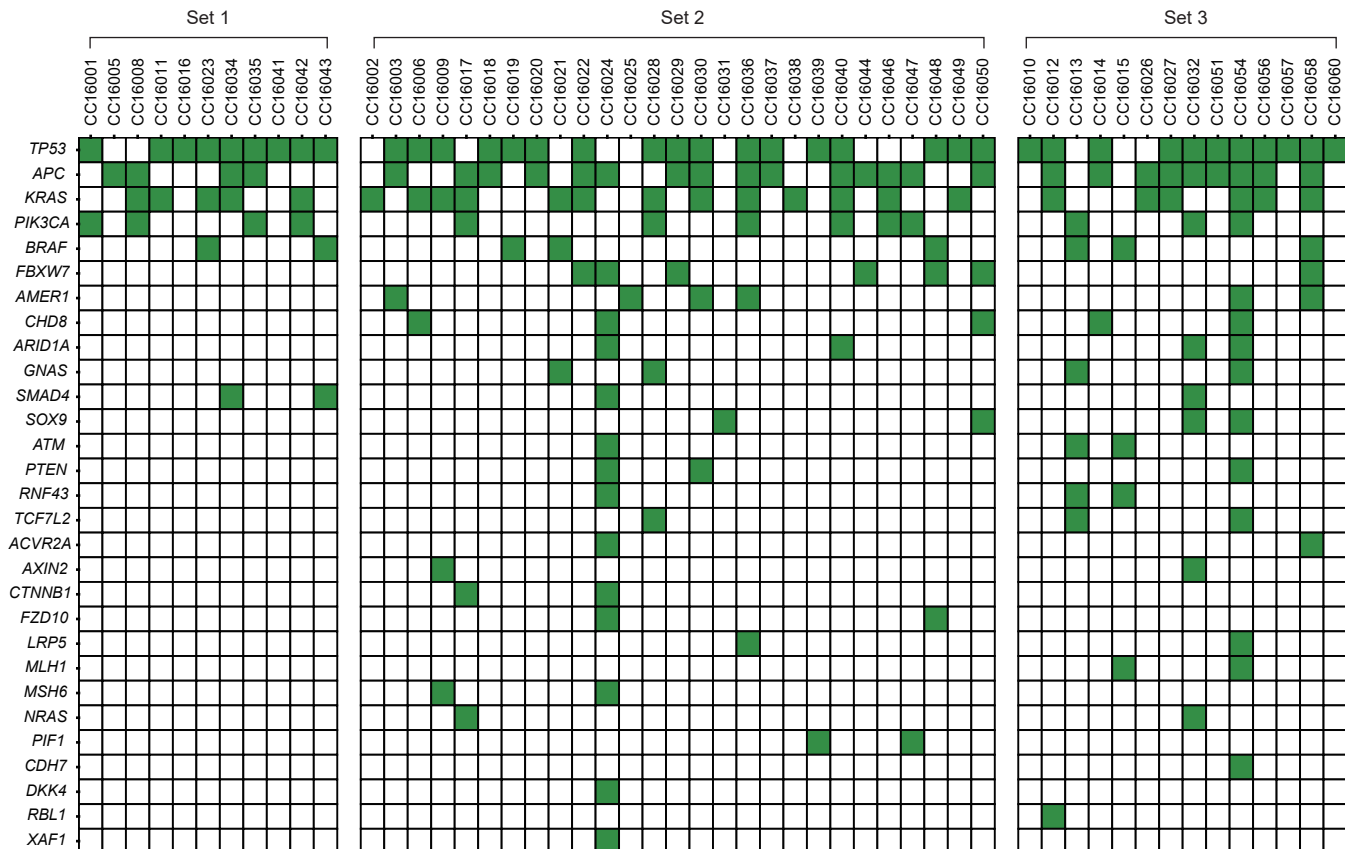
chr11:108229289	<i>ATM</i>	nonsynonymous	c.T297G	p.S99R	2543	1999	543	21.36			
chr7:140800366	<i>BRAF</i>	nonsynonymous	c.A976G	p.I326V	6118	2861	3254	53.17			
chr3:37025979	<i>MLH1</i>	stopgain	c.A658T	p.K220*	2536	1912	620	24.45			
chr17:58358121	<i>RNF43</i>	nonsynonymous	c.G1274A	p.R425H	7705	5986	1689	21.95			
chr17:58358788	<i>RNF43</i>	stopgain	c.C988T	p.R330*	1226	249	32	11.27	yes	2.43	
chr17:58363351	<i>RNF43</i>	nonsynonymous	c.C125A	p.A42D	2536	1912	620	24.45			
CC16026	chr5:112775687	<i>APC</i>	stopgain	c.C481T	p.Q161*	2430	1392	1027	42.21		
	chr12:25245350	<i>KRAS</i>	nonsynonymous	c.G35A	p.G12D	7144	5172	1967	27.54	yes	0
CC16027	chr5:112839942	<i>APC</i>	stopgain	c.C4348T	p.R1450*	3185	2036	1148	36.02		
CC16027	chr12:25245350	<i>KRAS</i>	nonsynonymous	c.G35T	p.G12V	5261	3070	2188	41.6	yes	0
	chr17:7675180	<i>TP53</i>	frameshift insertion	c.35_36insTGCA	p.Q12Hfs*6	2962	1151	1804	60.42	yes	0.27
CC16032	chr5:112839879	<i>APC</i>	stopgain	c.C4285T	p.Q1429*	2611	1315	1265	48.37		
	chr1:26772550	<i>ARID1A</i>	frameshift deletion	c.3458delC	p.M1154Wfs*7	2596	1311	1291	49.43		
	chr17:65537787	<i>AXIN2</i>	nonsynonymous	c.G1249T	p.A417S	2424	1763	518	22.7		
	chr1:114713909	<i>NRAS</i>	nonsynonymous	c.C181A	p.Q61K	3255	2100	1053	33.31	yes	21.6
	chr3:179218303	<i>PIK3CA</i>	nonsynonymous	c.G1633A	p.E545K	1015	766	249	24.53	yes	11.8
	chr18:51078425	<i>SMAD4</i>	frameshift deletion	c.1618delC	p.L540Ffs*12	2693	1435	1279	47.02		
	chr17:72121597	<i>SOX9</i>	frameshift deletion	c.207delC	p.V71Cfs*39	2040	1510	462	22.42		
	chr17:7673763	<i>TP53</i>	frameshift deletion	c.460delG	p.E154Kfs*59	1751	856	899	51.17	yes	0.19

CC16051	chr5:112839117	APC	stopgain	c.C3523T	p.Q1175*	4098	3380	707	17.21		
	chr17:7675088	TP53	nonsynonymous	c.G524A	p.R175H	7057	6177	872	12.34	yes	0.31
	chrX:64192215	AMER1	stopgain	c.C1072T	p.R358*	3751	770	2980	79.42		
	chrX:64191813	AMER1	frameshift insertion	c.1473dupC	p.R492Qfs*16	1573	1447	372	20.26		
	chrX:64191986	AMER1	frameshift insertion	c.1300dupC	p.H434Pfs*7	499	265	268	49.91		
	chrX:64192785	AMER1	frameshift insertion	c.501dupA	p.G168Rfs*7	287	141	193	57.78		
	chrX:64193123	AMER1	frameshift insertion	c.163dupA	p.T55Nfs*17	2999	2365	707	22.91		
	chr5:112838455	APC	stopgain	c.T2861A	p.L954*	4502	2996	1494	33.11		
	chr5:112840155	APC	stopgain	c.G4561T	p.E1521*	3346	2651	682	20.36		
	chr5:112840372	APC	nonsynonymous	c.A4724G	p.K1575R	645	566	77	11.94		
CC16054	chr5:112841875	APC	nonsynonymous	c.C6281T	p.P2094L	4071	3606	461	11.32		
	chr5:112819329	APC	frameshift insertion	c.1244dupA	p.D416Gfs*10	941	711	296	29.37		
	chr5:112840383	APC	frameshift insertion	c.4736dupC	p.A1580Cfs*34	588	484	191	28.25		
	chr1:26773683	ARID1A	nonsynonymous	c.T3970C	p.Y1324H	1768	1573	187	10.56		
	chr1:26773685	ARID1A	stopgain	c.C3972A	p.Y1324*	1482	1238	204	14.14		
	chr1:26779587	ARID1A	nonsynonymous	c.C5689G	p.P1897A	1764	903	370	28.95		
	chr1:26774569	ARID1A	frameshift insertion	c.4343dupC	p.G1449Rfs*42	546	297	297	49.25		
	chr1:26774597	ARID1A	frameshift insertion	c.4371dupC	p.Q1458Pfs*33	634	390	267	40.39		
	chr1:26774620	ARID1A	frameshift insertion	c.4394dupC	p.A1466Cfs*25	830	643	236	26.85		

chr11:108244102	<i>ATM</i>	frameshift insertion	c.646_647insT	p.A216Vfs*38	1826	1183	626	33.23		
chr11:108281146	<i>ATM</i>	frameshift insertion	c.3555dupA	p.E1186Rfs*14	850	547	349	38.86		
chr8:60852937	<i>CHD7</i>	frameshift deletion	c.6213delC	p.Q2073Sfs*71	1740	1153	561	31.22		
chr8:60865588	<i>CHD7</i>	frameshift insertion	c.2503dupC	p.S836Lfs*56	1880	801	1108	57.29		
chr14:21391024	<i>CHD8</i>	stopgain	c.A7105T	p.K2369X	1101	937	150	13.57		
chr20:58853838	<i>GNAS</i>	nonsynonymous	c.T386C	p.L129P	2997	1550	1441	48.03		
chr12:25245350	<i>KRAS</i>	nonsynonymous	c.G35A	p.G12D	7392	3692	3700	50.05	yes	0
chr12:25225691	<i>KRAS</i>	frameshift insertion	c.372dupA	p.V125Sfs*19	837	601	337	35.93		
chr11:68390006	<i>LRP5</i>	frameshift insertion	c.1539dupG	p.E514Gfs*20	818	603	244	28.74		
chr11:68403698	<i>LRP5</i>	frameshift insertion	c.1801dupG	p.T602Nfs*35	317	235	88	27.16		
chr11:68425992	<i>LRP5</i>	frameshift insertion	c.1699_1700insG	p.T567Sfs*73	1545	953	714	41.34		
chr3:37025946	<i>MLH1</i>	nonsynonymous	c.G625A	p.D209N	2946	2222	721	24.47		
chr3:37025947	<i>MLH1</i>	nonsynonymous	c.A626G	p.D209G	4189	3242	725	17.1		
chr3:37050487	<i>MLH1</i>	stopgain	c.1899dupT	p.E634*	2225	1589	1217	43.28		
chr3:179204536	<i>PIK3CA</i>	nonsynonymous	c.G1093A	p.E365K	1706	1190	508	29.85		
chr10:87952121	<i>PTEN</i>	frameshift insertion	c.497dupT	p.T167Nfs*13	3258	2607	854	24.64		
chr17:72124335	<i>SOX9</i>	frameshift insertion	c.1479dupC	p.S494Qfs*84	3009	2262	857	27.25		
chr10:13141234	<i>TCF7L2</i>	frameshift insertion	c.175dupC	p.L60Sfs*7	2834	2365	1314	35.39		
chr17:7675140	<i>TP53</i>	nonsynonymous	c.C472T	p.R158C	2243	1395	846	37.72		

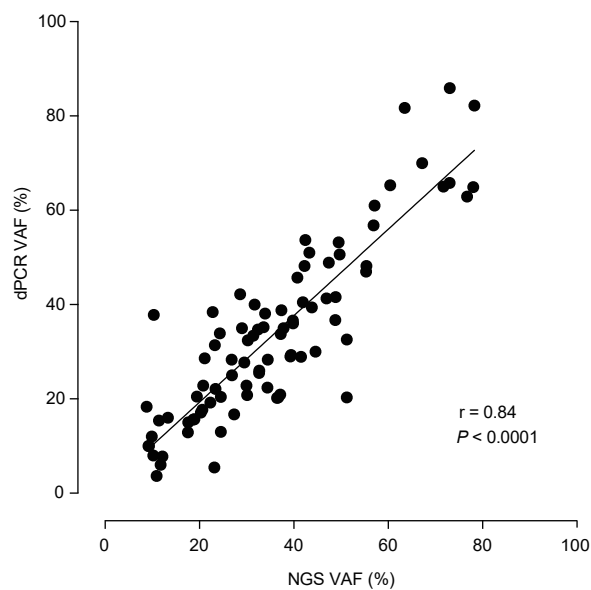
	chr5:112838007	<i>APC</i>	stopgain	c.C2413T	p.R805*	3842	3363	473	12.32		
CC16056	chr12:25245350	<i>KRAS</i>	nonsynonymous	c.G35C	p.G12A	7850	5479	2367	30.15	yes	0.43
	chr17:7673776	<i>TP53</i>	nonsynonymous	c.C844T	p.R282W	2675	1866	807	30.17	yes	0.11
CC16057	chr17:7674894	<i>TP53</i>	stopgain	c.C637T	p.R213*	6914	5266	1456	21.14	yes	0
	chr17:7675237	<i>TP53</i>	splicing	c.376-1G>A		2716	2013	703	25.87		
	chr2:147926138	<i>ACVR2A</i>	nonsynonymous	c.A1000G	p.R334G	828	721	107	12.92		
	chrX:64192583	<i>AMER1</i>	nonsynonymous	c.C704T	p.P235L	250	42	34	44.74		
CC16058	chr5:112780895	<i>APC</i>	stopgain	c.C637T	p.R213*	3101	2512	583	18.78		
	chr7:140924640	<i>BRAF</i>	nonsynonymous	c.G64A	p.D22N	3979	1662	2299	58.04		
	chr4:152328232	<i>FBXW7</i>	nonsynonymous	c.G1394A	p.R465H	7171	5373	1796	25.03		
	chr12:25245350	<i>KRAS</i>	nonsynonymous	c.G35C	p.G12A	7807	6214	1591	20.38	yes	0
	chr17:7673775	<i>TP53</i>	nonframeshift insertion	c.448_449insACC	p.D149_R150insH	3013	2195	813	26.89	yes	2.05
CC16060	chr17:7673802	<i>TP53</i>	nonsynonymous	c.G818A	p.R273H	6995	1890	5098	72.85	yes	1.22

<sup>a</sup> Variant allele frequency,<sup>b</sup> Plasma DNA was evaluated by dPCR,<sup>c</sup> Variant circulating tumor DNA

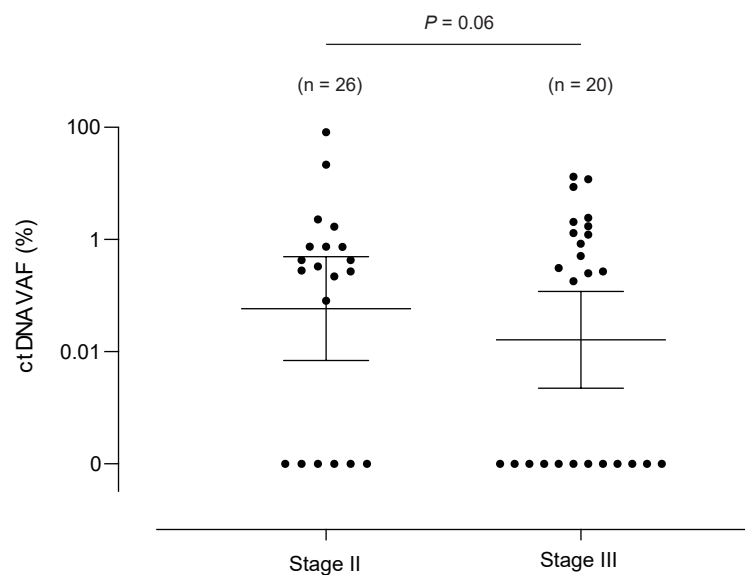


**Supplementary Figure 1. Somatic mutation profile of primary CRC tumors from the 52 patients in the study cohort.**

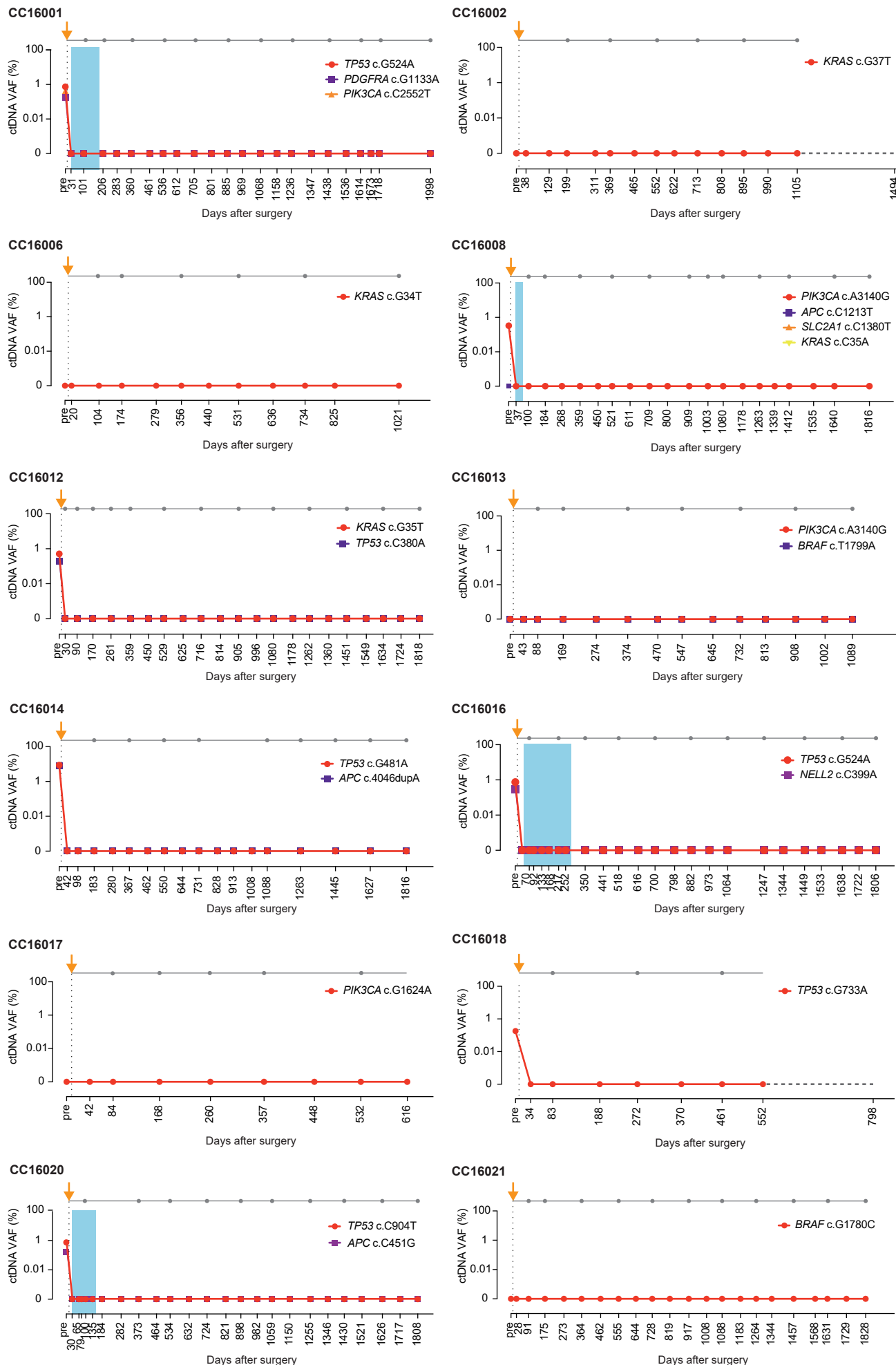
Mutated genes that satisfied the criteria of each set are shown. The top row indicates the patient ID. Genes listed in the custom panel (Supplementary Table S2) are arranged on the left side of the panel. The detailed mutation profile for Set 1 is available in our previous report (Ref. 31 in the main text). Green boxes indicate the presence of mutations.

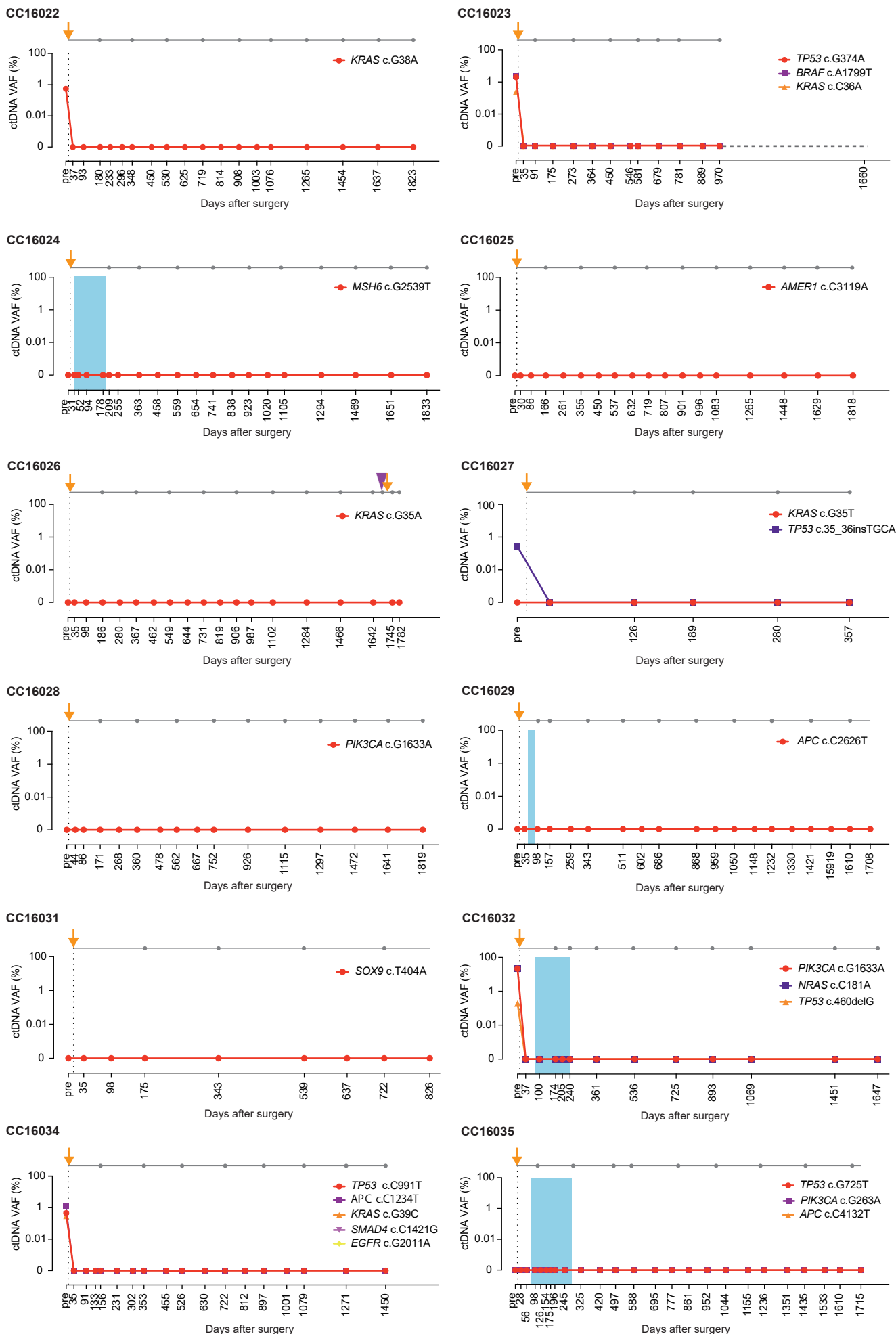
**Supplementary Figure 2. Correlation between primary tumor VAFs measured by NGS and dPCR.**

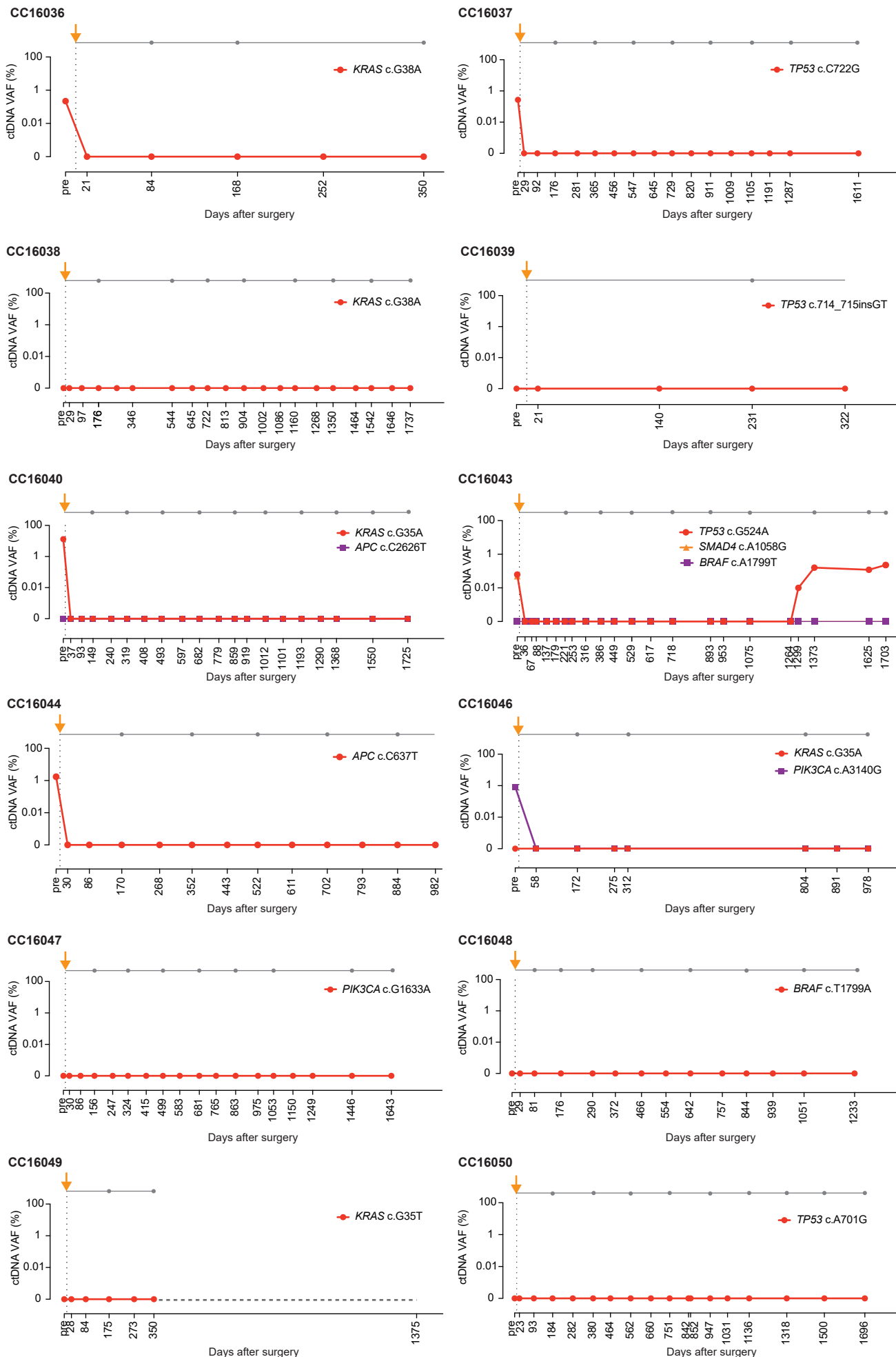
Strong positive correlations between NGS and dPCR VAFs were observed in primary tumor DNA ( $r = 0.84$ , Spearman's rank correlation coefficient). VAF, variant allele frequency; NGS, next generation sequencing; dPCR, digital PCR.

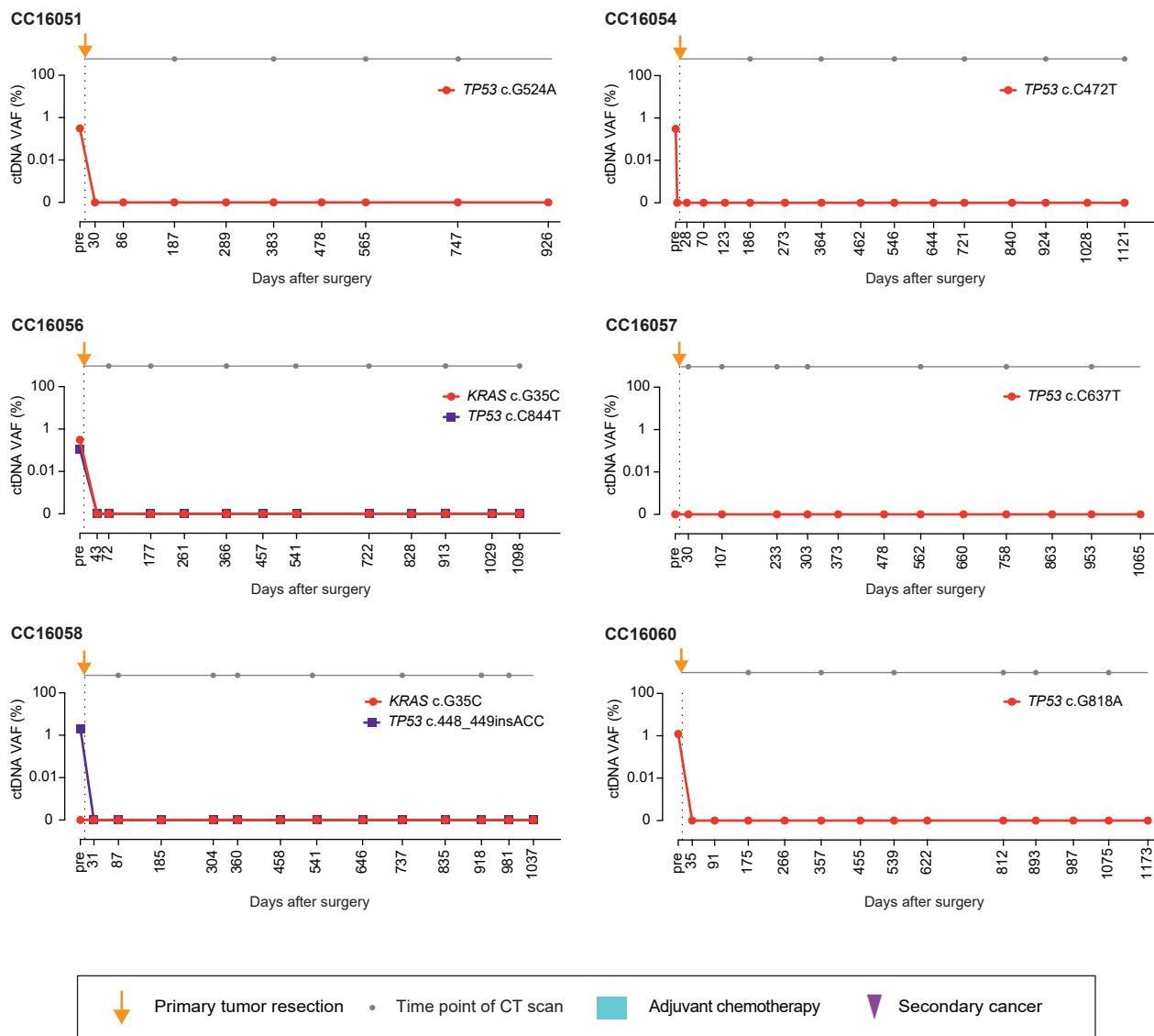


**Supplementary Figure 3. Pretreatment levels of ctDNA in patients with stage II and III CRC.**  
ctDNA, circulating tumor DNA; VAF, variant allele frequency.

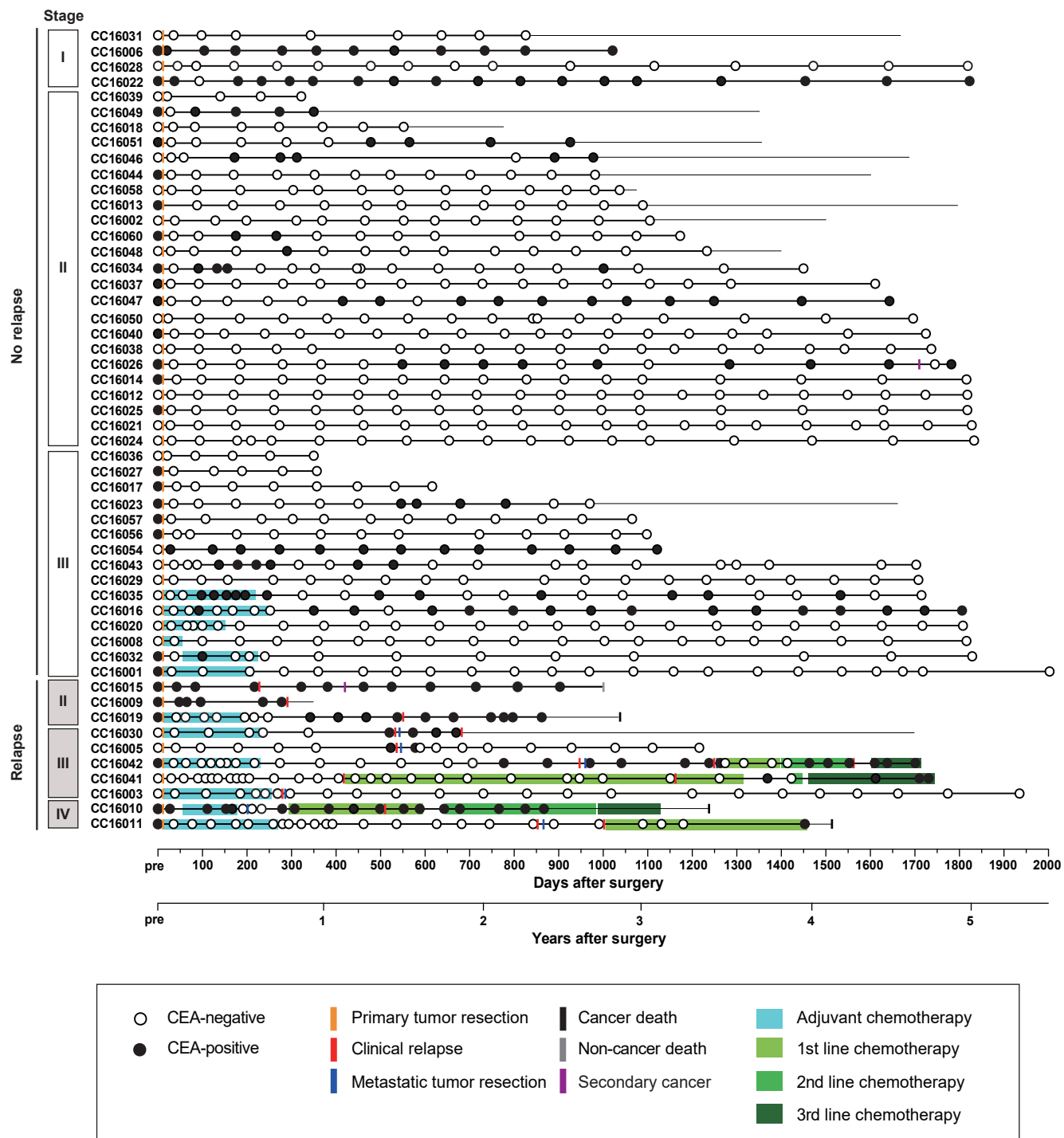




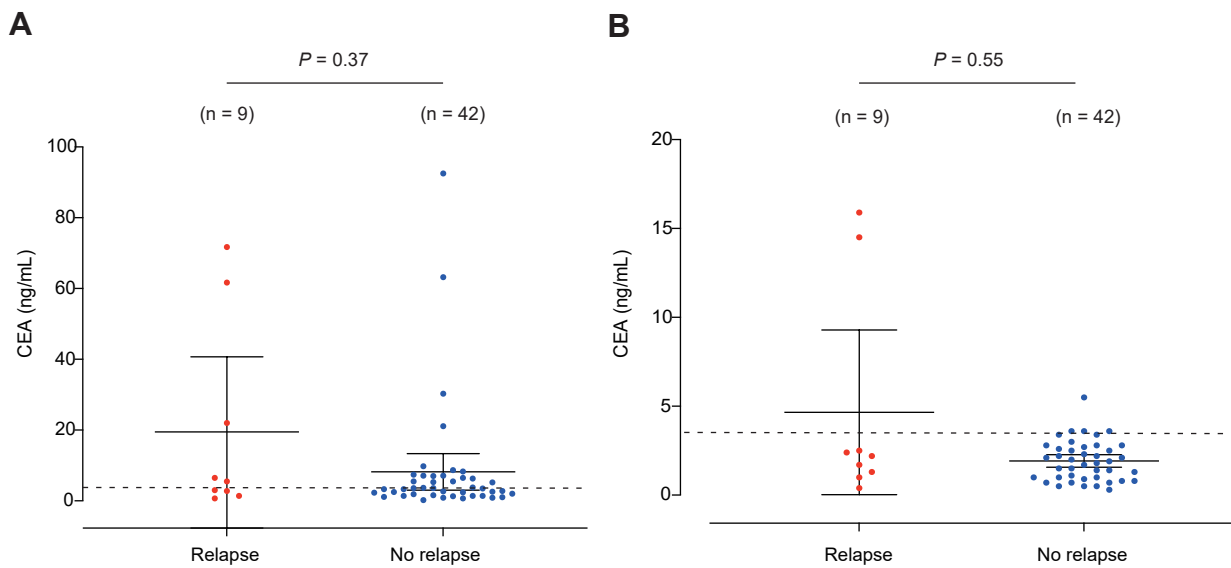




**Supplementary Figure 4. Dynamics of ctDNA in 42 patients with CRC without clinical relapse.**  
VAF, variant allele frequency.

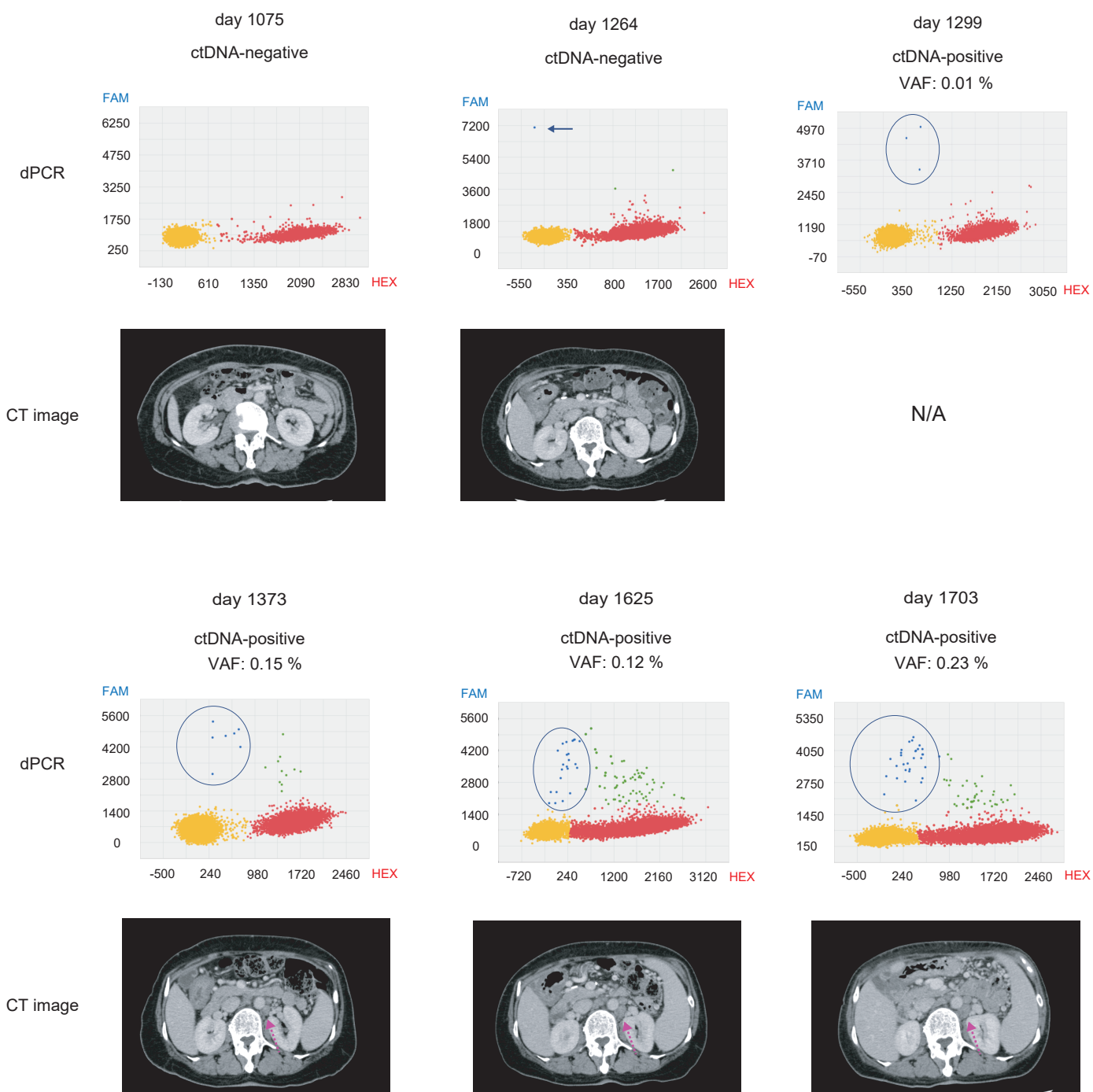


**Supplementary Figure 5. Longitudinal CEA monitoring during the postoperative period in patients with CRC.**  
CEA, carcinoembryonic antigen.



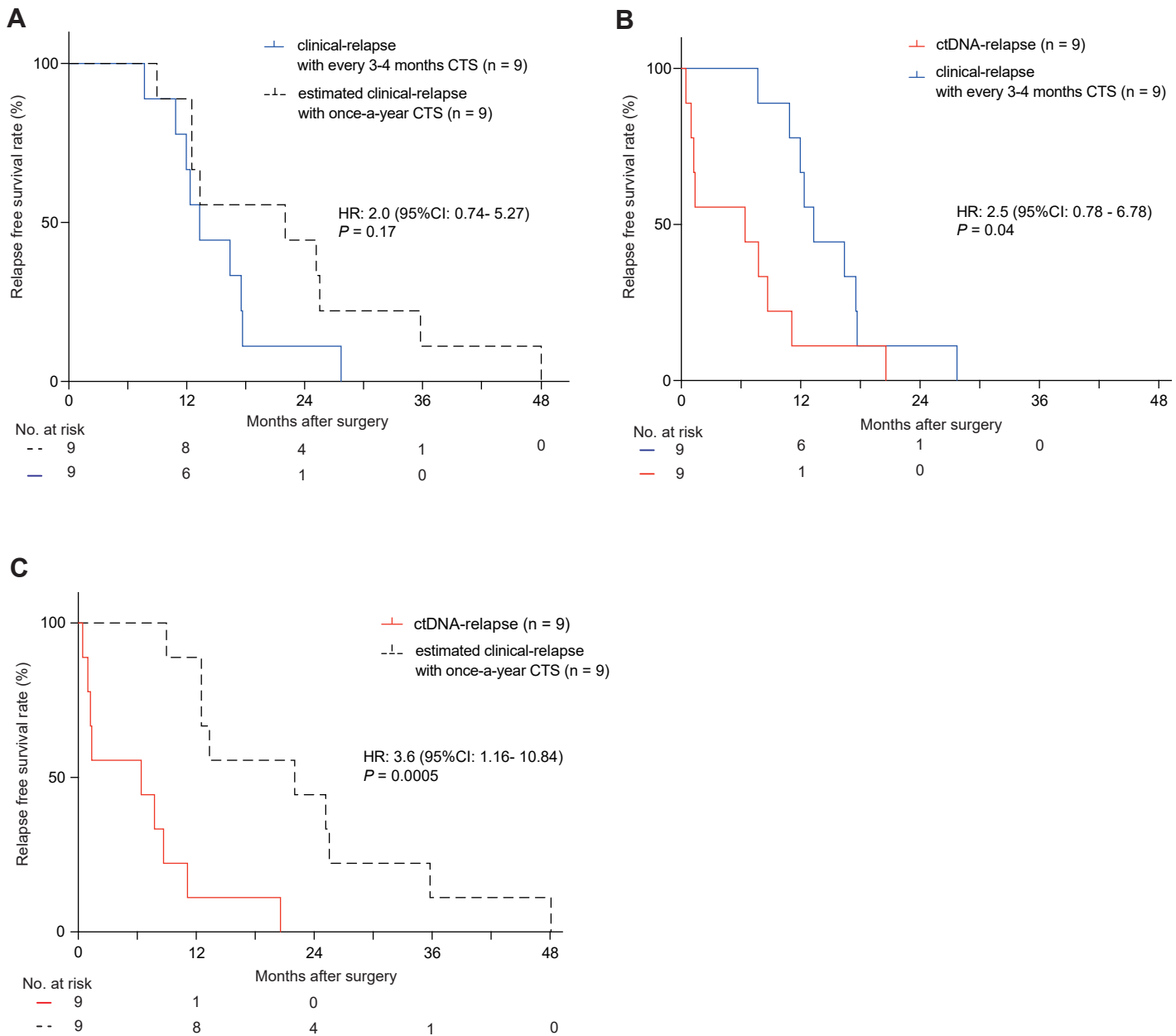
**Supplementary Figure 6. Association between CEA status and clinical relapse.**

(A) Preoperative and (B) postoperative levels of CEA in CRC patients with and without relapse. Plasma samples at the first postoperative time point were collected an average of 34.0 days (range, 20-58) after curative resection. Broken lines indicate the upper limit of normal levels for CEA (3.4 ng/mL). CEA, carcinoembryonic antigen.



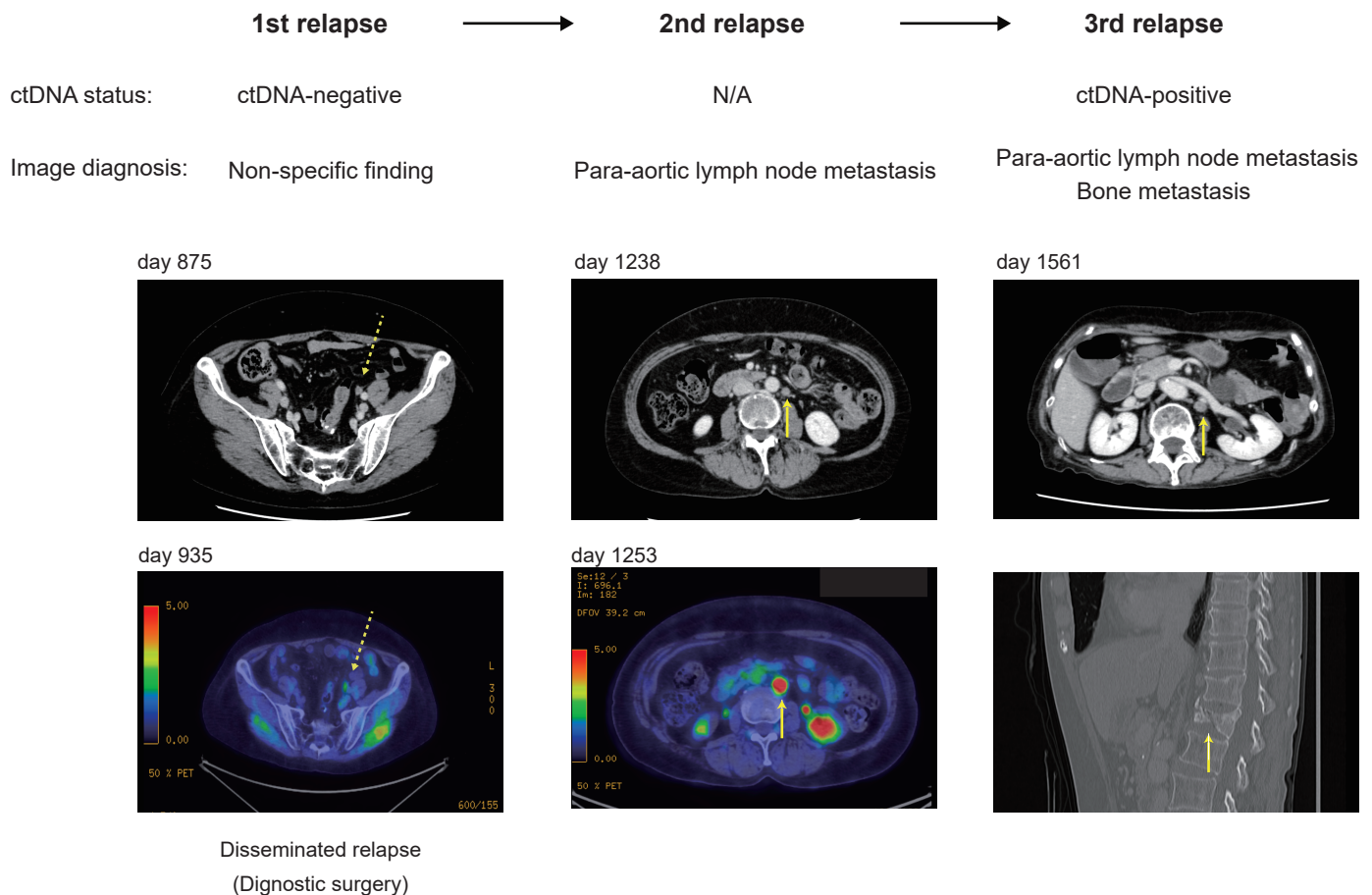
#### Supplementary Figure 7. Results of ctDNA analyses and corresponding CT images for Patient CC16043.

Results of ctDNA analyses by dPCR at postoperative time points are shown in the upper panels. Red and blue dots indicate wild-type and mutant reactions for a specifically designed primer/probe set for the tumor-specific mutation (*TP53* c.G524A). CT images corresponding to the timing of dPCR analysis are shown in the lower panels. Although one positive reaction for a mutation was observed on day 1,264 (arrow), no positive reactions for the mutation were detected upon retesting. Therefore, the ctDNA status of this time point was defined as ctDNA negative (see Supplementary Methods). From days 1,299 to 1,703, ctDNA VAF levels showed an increasing trend (blue circles). Red arrows in the bottom panels of the CT images indicate a non-specific para-aortic lesion, which was not confirmed as relapse. dPCR, digital PCR; ctDNA, circulating tumor DNA; VAF, variant allele frequency; CT, computed tomography; N/A, not applicable.



**Supplementary Figure 8. Comparison of relapse free survival (RFS) rates according to relapse type.**

(A) Clinical-RFS rates with CTS every 3-4 months and estimated clinical-RFS with once-a-year CTS. (B) Clinical-RFS and ctDNA-RFS rates. (C) Estimated clinical-RFS with once-a-year CTS and ctDNA-RFS rates. P values were derived using the Kaplan-Meier log-rank test. HR was calculated using the log-rank test. HR, ctDNA, circulating tumor DNA; CTS, computed tomography scan; HR, hazard ratio.



**Supplementary Figure 9. Images of recurrent tumors in Patient CC16042.**

Left panels, Non-specific findings of an intrapelvic small lesion on CTS and PET/CT. The lesion was pathologically diagnosed as a disseminated relapse after diagnostic surgery (first relapse). Middle panels, Para-aortic lymph node metastasis on CTS and PET/CT (second relapse). Right panels, Metastases of para-aortic lymph node and bone (third relapse). After surgical resection of the metastasis at the time of second relapse, continuous ctDNA positivity was observed until the third relapse (see Figure 4). Dashed arrows indicate non-specific imaging findings. Solid arrows indicate imaging-confirmed metastasis. CTS, computed tomography scan; PET, positron emission tomography; ctDNA, circulating tumor DNA.